1960-04

Numerical Prognosis Including Non-Adiabatic Warming

Haltiner, G.J.

Journal of Meteorology, Volume 17, pp. 207-213, April 1960.
http://hdl.handle.net/10945/45772

NUMERICAL PROGNOSIS INCLUDING NON-ADIABATIC WARMING

G. J. Haltiner

United States Naval Postgraduate School

AND

Lcdr. Yeh-chun Wang, RCN

Chinese Naval Postgraduate School, Taiwan

(Manuscript received 5 June 1959)

ABSTRACT

A model for numerical prediction of the 1000-mb surface is developed which includes a term expressing the interchange of sensible heat between the air and the underlying surface as well as the effect of terrain-induced vertical motion. In spite of the crudeness of the non-adiabatic representation, the model shows a definite improvement over a similar adiabatic model when the two are compared in a series of prognoses. Moreover, when monthly mean isotherms may be used to represent the temperature of the underlying surface, the non-adiabatic term may be combined with the orographic term and the earth's vorticity so that there is no work added to the prognostic routine.

1. Introduction

Considerable success has been achieved in the preparation of prognostic charts of the pressure field by the numerical solution of the dynamical equations. Most of the models assume that the air is dry and its motion is adiabatic. This assumption is based on the fact that many non-adiabatic processes appear to act rather slowly and may be reasonably neglected for short-range forecasts of the large-scale pressure field. Moreover, the inclusion of non-adiabatic influences may complicate the system of hydrodynamic equations considerably, thus hindering their solution or at least lengthening the time required for solution.

Nevertheless, in certain instances, there is a very rapid addition of heat to an air mass through turbulent diffusion from a warm underlying surface. A notable example is found in the transformation of a continental polar air mass as it acquires maritime characteristics. Here, and even in less striking cases, the non-adiabatic influences may cause significant errors in the prognoses obtained by adiabatic models.

Recently, Reed [5] adapted Burke's [1] treatment of the *cP* air-mass modification to a numerical-graphical technique for the prognosis of the 1000-mb surface. His results showed improvement over a similar adiabatic model in a single example that was presented for illustrative purposes. However, the method appears to lengthen appreciably the time required to prepare a prognosis.

It is the purpose of this paper to present an inexact, but extremely simple, method of including the non-adiabatic exchange of sensible heat between an air mass and the underlying surface in a numerical prediction model for the 1000-mb surface. As a result of the simplicity, there is essentially no added work in the preparation of a prognostic chart when the non-adiabatic effect is included; yet, in the cases tested, the non-adiabatic model shows a definite improvement over the corresponding adiabatic model.

2. The prediction equation

The development here parallels an earlier investigation [3] in which the effect of terrain-induced vertical motions was incorporated into a model for 1000-mb prognosis. The reader is referred to this article for further details on the derivation of the necessary equations, which will be presented in rather abbreviated form here.

When combined with the continuity equation, the vorticity equation may be written in (x, y, p, t) coordinates in the approximate form

$$\frac{\partial \zeta}{\partial t} + V\cdot\nabla(\zeta + f) = f\frac{\partial \omega}{\partial p}, \tag{1}$$

where ζ is the relative vorticity, f the Coriolis parameter, V the horizontal wind, ∇ is the horizontal "del" operator as applied on a constant-pressure surface, and $\omega = dp/dt$ is the individual rate of change of pressure. The last named variable is assumed to have a large-scale parabolic distribution [4] with a superimposed terrain-induced vertical motion as follows:

$$\omega(x, y, p, t) = \omega_5(x, y, t)\left[1 - \left(\frac{p - p_5}{p_0 - p_5}\right)^2\right] - g\rho_0 k_1 \frac{p}{p_0} V_0\cdot\nabla H. \tag{2}$$

Here the subscripts 0 and 5 refer to the 1000-mb and 500-mb levels, respectively; ρ_0 is the density, g is gravity, k_1 is a constant and H is the terrain height. In arriving at the orographic term, it is assumed that the vertical velocity w_0 at 1000 mb is proportional to the product of the horizontal wind velocity and the gradient of terrain height—*i.e.*,

$$w_0 = k_1 V_0 \cdot \nabla H,$$

and moreover that the terrain-induced vertical velocity decreases linearly with pressure. Finally, as a good approximation,

$$\omega \doteq -g\rho w.$$

Thus, we arrive at the last term constituting ω in eq (2).

Next the derivative of eq (2) is substituted into eq (1) and the result evaluated at p_0, giving the vorticity equation for this level as

$$\frac{\partial \zeta_0}{\partial t} + V_0 \cdot \nabla(\zeta + f) = -\frac{2f\omega_5}{p_5} - \frac{g\rho_0 f k_1}{p_0} V_0 \cdot \nabla H; \quad (3)$$

a second equation involving ω_5 may be obtained from the first law of thermodynamics which is expressible in the form

$$\frac{dQ}{dt} = c_p \frac{T}{\theta}\frac{d\theta}{dt}, \quad (4)$$

where Q is the heat added, c_p the specific heat or constant pressure, T the temperature, and θ the potential temperature. The last equation shows that the rate of heat gain or loss is proportional to the individual rate of change of potential temperature. The latter may be expanded in (x, y, p, t) coordinates to yield

$$\frac{1}{\theta}\frac{d\theta}{dt} = \frac{1}{\theta}\frac{\partial \theta}{\partial t} + \frac{1}{\theta} V \cdot \nabla\theta + \frac{1}{\theta}\omega\frac{\partial\theta}{\partial p}. \quad (5)$$

It follows from Poisson's equation,

$$\theta = \frac{p\alpha}{R}\left(\frac{p_0}{p}\right)^{R/c_p},$$

that the first two terms on the right side of eq (5) may be replaced by $(1/\alpha)(\partial\alpha/\partial t)$ and $(1/\alpha)(V\cdot\nabla\alpha)$ respectively. Here R is the gas constant for air. Finally, the specific volume in these two terms may be removed by the use of the hydrostatic equation, $\alpha = -g(\partial Z/\partial p)$. The result is the so-called thermal equation

$$\frac{1}{g}\frac{\alpha}{\theta}\frac{d\theta}{dt} = -\frac{\partial}{\partial t}\left(\frac{\partial Z}{\partial p}\right) - V\cdot\nabla\left(\frac{\partial Z}{\partial p}\right) - \sigma\omega. \quad (6)$$

Here Z is the height of a constant-pressure surface, and σ is the stability parameter

$$\sigma = -\frac{\alpha}{g\theta}\frac{\partial\theta}{\partial p}.$$

Now consider the gain of heat by an air mass as it moves over warmer water. The surface air temperature quickly adjusts to that of the surface water and rapid vertical diffusion of heat takes place. The rate of diffusion will normally increase with increasing horizontal wind which enhances the turbulence and also will certainly continue as long as the surface water temperature increases. When a warm air mass moves over colder water, the loss of heat by the air normally takes place at a slower rate because of stability created by the surface cooling. In spite of such differences, we shall assume, as a rough estimate, that the rate of heat loss or gain is proportional to the expression $V_0\cdot\nabla T_s$, where T_s is the surface temperature of the underlying sea surface. This assumption will be discussed somewhat further in a later section; for the present, we shall proceed with the development. It follows that eq (6) may be written in the form

$$\frac{\partial}{\partial t}\left(\frac{\partial Z}{\partial p}\right) = -V\cdot\nabla\left(\frac{\partial Z}{\partial p}\right) - \sigma\omega - k_2 V_0\cdot\nabla T_s, \quad (7)$$

where k_2 is a constant of proportionality. Substituting for ω from eq (2) and integrating between p_0 and p_5 leads to the result

$$\frac{\partial h}{\partial t} = -V_0\cdot\nabla h + \tfrac{2}{3}p_5\sigma\omega_5 - \tfrac{3}{4}g\rho_0 p_5 k_1\sigma V_0\cdot\nabla H + p_5 k_2 V_0\cdot\nabla T_s. \quad (8)$$

Here h is the 1000- to 500-mb thickness, and σ is assumed constant. The above equation may be solved for ω_5 and substituted into eq (3). Neglecting horizontal variations in ρ_0 and f where they appear as coefficients of h, H and T_s, we obtain

$$\frac{\partial\zeta_0}{\partial t} + \frac{3f}{\sigma p_5^2}\frac{\partial h}{\partial t} = -V_0\cdot\nabla\left(\zeta_0 + f + \frac{11\rho_0 g f k_1}{2p_0}H + \frac{3f}{\sigma p_5^2}h - \frac{3fk_2}{\sigma p_5}T_s\right). \quad (9)$$

Now we make the geostrophic, finite-difference approximation for the vorticity

$$\zeta_0 = \frac{4gm^2}{fd^2}(\bar{Z}_0 - Z_0),$$

where m is the map-scale factor and d is the grid distance. Substitution of this expression into eq (9), and following Fjørtoft by neglecting the variation of m^2/f compared to $\bar{Z}_0 - Z_0$, gives

$$\frac{\partial}{\partial t}(\bar{Z}_0 - Z_0 + Ch + G + F + NT_s) = -V_0\cdot\nabla(\bar{Z}_0 - Z_0 + Ch + G + F + NT_s), \quad (10)$$

where

$$C = \frac{3f^2d^2}{4gm^2p_5^2\sigma}; \qquad G = \int_0^{\varphi} \frac{d^2\Omega^2}{gm^2} \sin\varphi\cos\varphi d\varphi;$$
$$F = \frac{11f^2d^2\rho_0 g k_1}{8m^2p_0}; \qquad N = -\frac{3k_2f^2d^2}{4gm^2\sigma p_5}. \tag{11}$$

The sea-surface temperature T_s varies slowly with time but usually may be assumed constant for the normal forecast periods of 24 to 48 hr. Thus the term NT_s, together with G and F, has been inserted in the left side of eq (10). This equation shows that the quantity $(\bar{Z}_0 - Z_0 + Ch + G + F + NT_s)$ is conservative with respect to the wind field at p_0. With the geostrophic approximation for V_0, eq (10) may be written in Jacobian form as

$$\frac{\partial}{\partial t}(\bar{Z}_0 - Z_0 + Ch + G + F + NT_s)$$
$$= -\frac{g}{f}J(Z_0, \bar{Z}_0 - Z_0 + Ch + G + F + NT_s). \tag{12}$$

The wind field at 1000 mb varies rather rapidly with time, and advection with the initial wind field for periods of 12 or more hours will frequently lead to gross errors. In order to obtain a more conservative wind field for advection purposes, we may apply the Jacobian identity $J(A, B) = J(A + B, B)$ to eq (12), giving

$$\frac{\partial}{\partial t}(\bar{Z}_0 - Z_0 + Ch + G + F + NT_s)$$
$$= -\frac{g}{f}J[(\bar{Z}_0 + Ch + G + F + NT_s),$$
$$(\bar{Z}_0 - Z_0 + Ch + G + F + NT_s)]. \tag{13}$$

To obtain the 1000-mb height changes, advect the initial

$$(\bar{Z}_0 - Z_0 + Ch + G + F + NT_s)$$

field for a period of time Δt, say 12 or 24 hr, with the

$$(\bar{Z}_0 + Ch + G + F + NT_s)$$

field. Denoting the local change of the advected quantity as $-D$, we have

$$\Delta(\bar{Z}_0 - Z_0 + Ch + G + F + NT_s) = -D. \tag{14}$$

Since $\Delta G = \Delta F = \Delta(NT_s) = 0$ and $h = Z_5 - Z_0$,

$$\Delta(\bar{Z}_0 - (1 + C)Z_0 + CZ_5) = -D. \tag{15}$$

Hence,

$$\Delta Z_0 = A + \frac{1}{1 + C}\Delta\bar{Z}_0, \tag{16}$$

where

$$A = \frac{1}{1 + C}(D + C\Delta Z_5). \tag{17}$$

Taking the space average of (16) gives

$$\Delta\bar{Z}_0 = \bar{A} + \frac{1}{1 + C}\Delta\bar{\bar{Z}}_0.$$

Substituting this result back into eq (16), we obtain

$$\Delta Z_0 = A + \frac{1}{1 + C}\left(\bar{A} + \frac{1}{1 + C}\Delta\bar{\bar{Z}}_0\right). \tag{18}$$

This process may be repeated; after n times, the result is

$$\Delta Z_0 = A + \frac{1}{1 + C}\bar{A} + \cdots + \frac{1}{(1 + C)^{n+1}}\Delta\bar{\overset{n+1}{\cdots}}_0. \tag{19}$$

Fjørtoft has shown that the series (19) may be approximated by the expression

$$\Delta Z_0 \doteq A + \frac{2}{1 + C}\bar{A}. \tag{20}$$

In the cases tested in this investigation, it was found that the second term on the right side of eq (20) involving $\bar{A}$ can be neglected except in cases of marked change. Obviously, when the procedure is carried out manually by graphical methods, there will be a great saving of time when the approximation $\Delta Z_0 \doteq A$ can be used. If a high-speed electronic computer is available, eq (12) or (13) can be solved with much greater accuracy and the iteration carried out in shorter time steps.

It should be noted that to complete the 1000-mb prognosis a forecast of the 500-mb height change is needed. This may be obtained by any desired method; for example, the barotropic model may be used. However, since the primary objective of this investigation was to ascertain the nature of the non-adiabatic exchange of sensible heat, the observed 500-mb height changes were used in computing the 1000-mb height change.

3. Procedure

In order to provide a comparison with Reed's earlier results, the same case has been chosen for prognostication. Two other series were also chosen for testing purposes; each series contained three consecutive 12-hr periods. Except in the same case as Reed's where the prognosis without heating was already available, two prognoses were made each time, one omitting and the other including the heating effects. A discussion of the choice of constants will appear later. For the present, we merely list the following steps carried out for each prognosis:

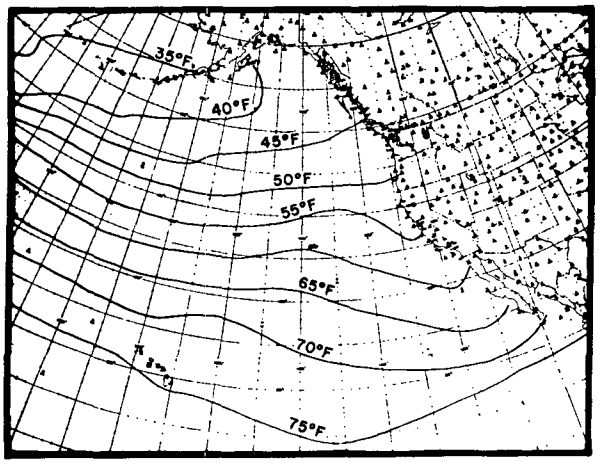

FIG. 1. Mean sea-surface isotherms for January.

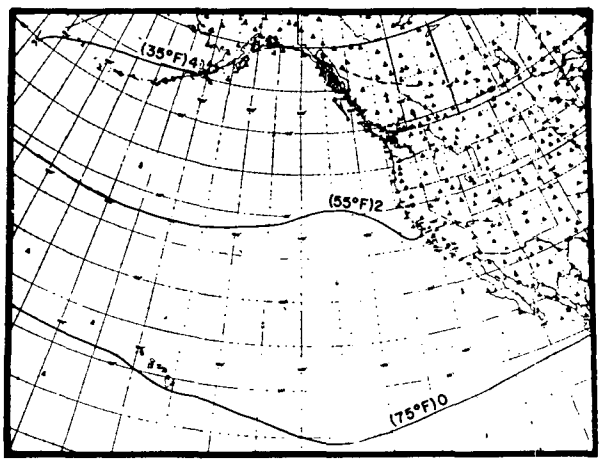

FIG. 2. The function NT_s in units of 100 ft for January. Numerical values are given relative to the value of at 75F.

(1) A space-mean of the initial Z_0 chart is graphically constructed using a grid distance of 600 km.
(2) With $C = 0.5$, the initial thickness values are divided by two (which is achieved by simply using every other line) and then added to $\bar{Z}_0$.
(3) Next, the result of step (2) is added to the function $(G + F)$ as provided in reference [3].
(4) With the appropriate value of N, the quantity NT_s is added to the result of step (3). As will be indicated later, this step may be combined with step (3) and carried out in a single operation under certain circumstances. Step (4) is omitted in the adiabatic case. The steps up through this stage have produced the stream chart with which the advecting is done by using the conventional geostrophic wind scale.
(5) Now Z_0 is subtracted from the stream chart of step (4).
(6) Next advect the quantity obtained in step (5) with the stream chart for the time interval of the forecast.
(7) Subtract the result of step (6) from step (5) to get D.
(8) Add $\frac{1}{2}\Delta Z_5$ to D and multiply by $\frac{2}{3}$ to get A.
(9) Obtain the space mean of A and multiply by $\frac{4}{3}$.
(10) Add the results of steps (8) and (9) to give ΔZ_0.

4. Discussion

In this investigation, three constants play a major role—namely, N, C and k_1. The last two of these have already been discussed in a previous paper [3]. Several values of C have been used by various investigators. In the present study, the value of $C = 0.5$ appeared to give the best results. Smaller values give too weak an advecting field, while larger values make the advecting field too strong.

Normally the sea-surface temperature changes rather slowly; hence, it was possible to use the monthly mean isotherms published by the Hydrographic Office (fig. 1) in the construction of the chart. An area of primary interest was in the vicinity of Alaska, for here air-mass modification was very pronounced. Over the ocean, the value of the constant N was empirically found to be approximately -10 ft per deg F. Air-mass modification, with the addition of sensible and also latent heat, is a complex process. The rate of heat diffusion is dependent upon a multitude of factors including (a) lapse rate, (b) wind speed, (c) sea conditions, (d) moisture content, *etc.* The interrelations between these various factors are not completely understood; hence, it is difficult to determine their relative importance in a specific case. For example, air moving at a high speed is not acquiring heat at exactly a proportionately higher rate than air moving at a low speed, as is implied by the expression $k_2 V_0 \cdot \nabla T_s$. Moreover, cold air tends to acquire heat more rapidly than a warm air mass loses heat to an underlying cold sea surface because of the instability created in the former through warming. Thus, the determination of N represents compromise of many influences. For the relatively small sample tested, the value $N = -10$ ft per deg F appears to be the best choice thus far. An attempt was made to advect less than the full distance in warm advection to offset the slower modification in the case of an air mass cooled from below; however, there was no overall improvement.

As indicated by eq (11), a given value of N, together with appropriate values of latitude, grid distance and stability parameter, determine a value of k_2. The constant of proportionality k_2, in accordance with eq (7), regulates the rate of addition of sensible heat. For example, with $N = -10$ ft per deg F, standard-atmosphere stability in middle latitudes, a

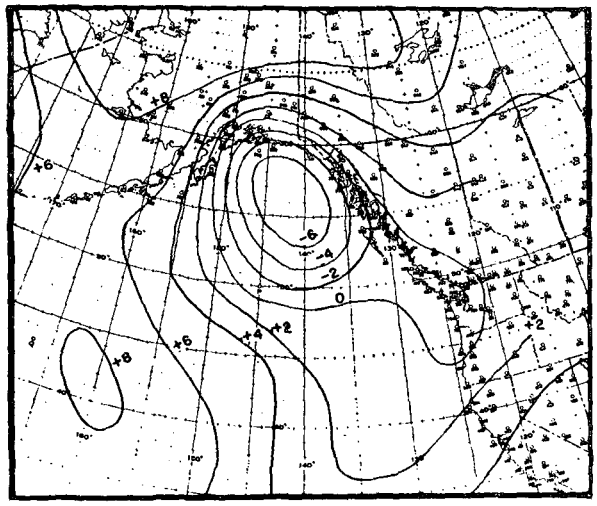

FIG. 3. The 1000-mb chart for 1500 GCT 4 January 1956.

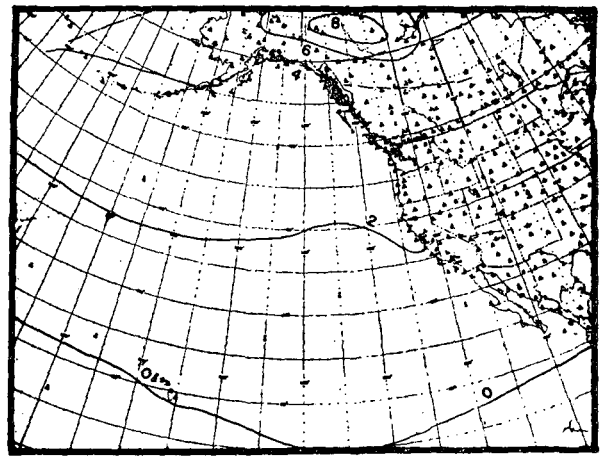

FIG. 4. The function NT_s in units of 100 feet based on sea-surface isotherms for January and the current temperatures over land areas for 1500 GCT 4 January 1956. Numerical values are given relative to the value of 75F.

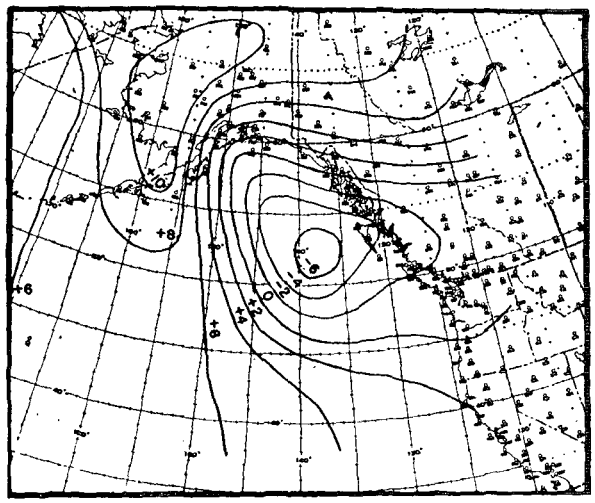

FIG. 5. The prognostic 1000-mb heights for 0300 GCT 5 January 1956, without the non-adiabatic term (after Reed [5]).

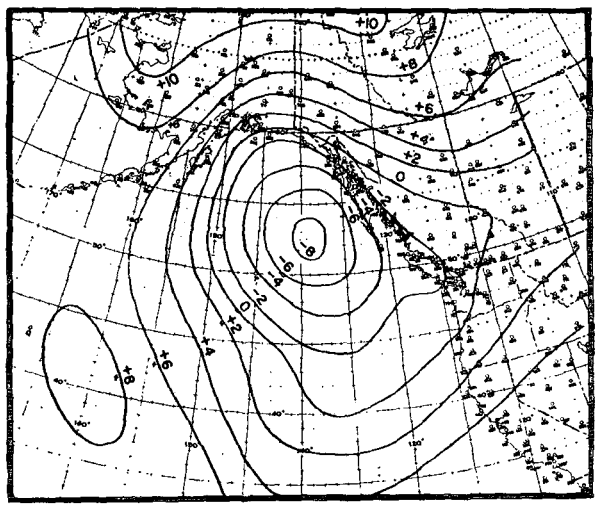

FIG. 6. The prognostic 1000-mb heights for 0300 GCT 5 January 1956, with the non-adiabatic term.

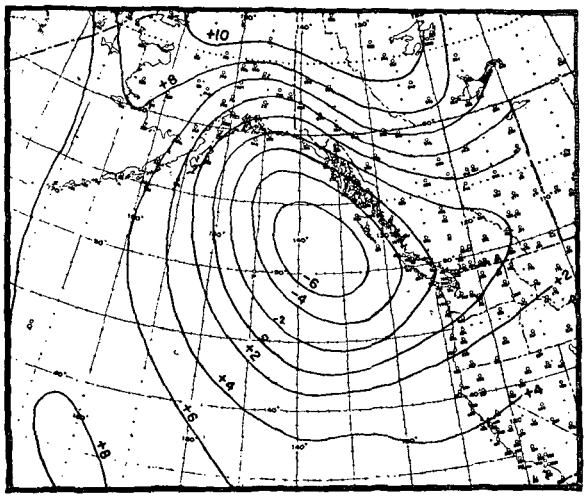

FIG. 7. The observed 1000-mb heights for 0300 GCT 5 January 1956.

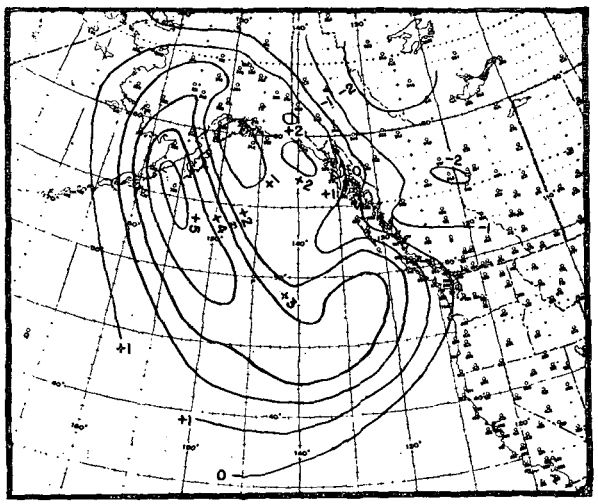

FIG. 8. Prognostic minus observed 1000-mb heights for 0300 GCT 5 January 1956, without the non-adiabatic term.

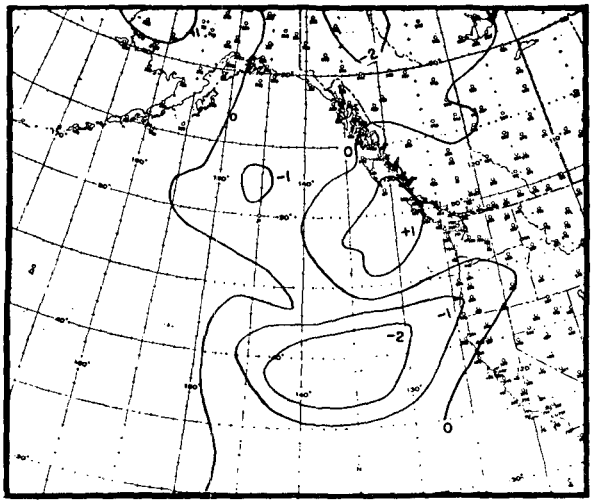

FIG. 9. Prognostic minus observed 1000-mb heights for 0300 GCT 5 January 1956, with the non-adiabatic term.

1000-mb wind of 20 m per sec and a surface temperature gradient of 2C per 100 km, the exchange of sensible heat is approximately 840 langlies per day, corresponding to a 1000- to 500-mb thickness change of about 400 ft per day. This value undoubtedly underestimates the heat gain by a cold air mass from a warm underlying surface but probably underestimates the heat loss by a warm air mass to a cold surface.

As a matter of fact, larger numerical values of N, say -20 ft per deg F, actually gave better results in the areas of strong cold advection. However, when considering more extensive areas containing both warm and cold advection, the numerically smaller value, $N = -10$ ft per deg F, gave better results. It should be noted that both values resulted in improvement over the analogous adiabatic model.

In the course of the experiment, it was noted that when the non-adiabatic term was omitted over Alaska the stream field tended to move the inland high-pressure cell downstream (westward in this case) when actually it remained nearly stationary. Since the non-adiabatic term would tend to offset this difficulty in a cold-high, an attempt was made to include the non-adiabatic term over a limited area of inland Alaska. The currently observed temperatures together with the value $N = -5$ ft per deg F were used to determine the NT_s field over land areas. Considerable improvement resulted. This suggests the use of a continuous temperature field over ocean and land alike; however, the examples provide a more limited test over the land areas than over oceans. A combined distribution of the quantity NT_s for 4 January 1956 is found in fig 4. For the particular cases investigated here, it appeared feasible to use the monthly mean temperatures over Alaska as well as those of the sea surface; however, this would certainly not be expected to apply over all land areas. When monthly mean isotherms are used, step (4) of the procedure can be combined with step (3) by preparing a single chart of $(G + F + NT_s)$ for each month. Thus, the orographic, non-adiabatic and the Coriolis terms of eq (13) are all accounted for in a single function. This represents a considerable saving of time, particularly when the prognosis is carried out manually by graphical techniques.

5. Results and conclusions

Prognoses were made with and without the non-adiabatic warming for the following cases:

Case 1: 1500 GCT 4 January 1956 to 0300 GCT 4 January 1956;

Cases 2, 3, 4: 0000 GCT 13 January 1959 to 1200 GCT 14 January 1959 consisting of 3 consecutive 12-hr prognoses;

Cases 5, 6, 7: 0000 GCT 13 January 1959 to 1200 GCT 14 January 1959.

Figs. 3 through 8 show some of the charts of case 1. Fig. 3 is the actual 1000-mb chart of case 1. Fig. 3 is the actual 1000-mb chart of 1500 GCT 4 January 1956. Fig. 4 is the chart of the quantity NT_s, including parts of Alaska and Canada where the function was determined from the smoothed isotherms of 4 January over the land area. Fig. 5 (after Reed) and fig. 6 show the prognostic charts for 0300 GCT 5 January 1956, without and with the non-adiabatic term, respectively. Fig. 7 shows the actual 1000-mb chart for 0300 GCT 5 January 1956. Fig. 8 shows the difference in hundreds of feet between the actual chart and the prognostic chart without the non-adiabatic term. Finally, fig. 9 gives the difference in hundreds of feet between the actual chart and the prognostic chart with the non-adiabatic term. Comparison of figs. 8 and 9 show that the greatest improvement is observed over the area of strong southward flow of cold air from Alaska over the Pacific Ocean.

The results of the test cases listed at the beginning of this section are summarized in table 1. Columns 2 and 3 give linear correlation coefficients between observed and forecast 1000-mb height changes, without and with the heating term respectively. Columns 4 and 5 give the root-mean-square error in feet, with and without the heating term. These statistical parameters were based on a grid of seventy points separated by 5-deg intervals extending from 120W to 165W and from 30N to 65N. Of the seventy points, 47 were over the sea and the remaining 23 were over land areas. Because of the convergence of meridians, the points are somewhat denser in the northern part of the areas, which included the land area and also the area of strongest influence of the non-adiabatic term. For comparison purposes, the results from land

TABLE 1. Summary of the results of test cases described in section 5.

Case	Correlation coefficient between observed and forecast 1000-mb height changes (70 points) heating omitted	heating included	RMS error (feet) heating omitted	RMS error (feet) heating included	Area
1500 GCT 4 January 1956 to 0300 GCT 5 January 1956	0.67*	0.89 (0.74*)	225*	(179*) 91.4	Total
			293*	(193*) 85	Ocean
0000 GCT 6 January 1959 to 1200 GCT 6 January 1959	0.69	0.78	133	115	Total
			126	109	Ocean
1200 GCT 6 January 1959 to 0000 GCT 7 January 1959	0.52	0.74	141	95	Total
			92	66	Ocean
0000 GCT 7 January 1959 to 1200 GCT 7 January 1959	0.66	0.79	147	67	Total
			105	68	Ocean
Average	0.635	0.80	161.5	92	Total
			154	82	Ocean

* After Reed [5]. RMS error in units of feet.

and ocean areas are separated. In case 1, the statistical parameters from Reed's method are included, as well as the results from the present investigation. The correlation coefficients between the prognostic and observed height changes and the root-mean-square errors show that in the cases tested there was a definite improvement in the prognoses when the non-adiabatic influence is included in the forecasting technique. In the foregoing cases, considerable modification of the air mass was expected. Subsequent to these tests, one other case at somewhat lower latitudes in the central Pacific Ocean was analyzed. Here the air-mass modification was far less pronounced and there was no significant difference between the prognoses with and without the non-adiabatic term.

It would be desirable to apply this technique on a daily operational basis, which would not only provide further testing but also, through a statistical analysis, might furnish a better choice of the parameter N. Such testing could be carried out most rapidly by means of an electronic computer rather than manually by graphical techniques. In brief, this investigation suggests the inclusion of a term of the form $V_0 \cdot \nabla T_s$ in the thermal equation of numerical forecasting systems to give a rough estimate of the exchange of sensible heat between the air mass and the underlying surface. An appropriate coefficient, not necessarily a constant, should be statistically determined to give the best results. In the model used here, there is no equation for the prediction of surface temperature; hence, the method can only be applied over areas where the surface temperature is fairly stable during the forecast period.

BIBLIOGRAPHY

1. Burke, C. J., 1945: Transformation of polar continental air to polar maritime air. *J. Meteor.*, **2**, 94–113.
2. Fjørtoft, R., 1952: On numerical method of integrating the barotropic vorticity equation. *Tellus*, **4**, 179–194.
3. Haltiner, G. J., and T. S. Hesse, 1958: Graphical prognosis including terrain effects. *J. Meteor.*, **15**, 103–107.
4. Kuo, H.-L., 1953: The stability properties and structure of disturbances in a baroclinic atmosphere. *J. Meteor.*, **10**, 235–243.
5. Reed, R. J., 1958: A graphical prediction model incorporating a form of non-adiabatic heating. *J. Meteor.*, **15**, 1–8.